Published in: Macromolecular Rapid Communications (2018), vol. 39, n°17, 1700814
DOI: 10.1002/marc.201700814
Status: Postprint (Author's version)

COMPLEX COACERVATE CORE MICELLES CONTAINING POLY(VINYL ALCOHOL) INHIBIT ICE RECRYSTALLIZATION

Christian C. M. Sproncken [a,b], Romà Surís-Valls [a,c], Hande E. Cingil [a,c], Christophe Detrembleur [d], and Ilja K. Voets [a,b,c]

[a] *Laboratory of Self-Organizing Soft Matter, Institute for Complex Molecular Systems, Eindhoven University of Technology, Post Office Box 513, 5600 MD, Eindhoven, The Netherlands*
[b] *Laboratory of Physical Chemistry, Department of Chemical Engineering and Chemistry, Eindhoven University of Technology, Post Office Box 513, 5600 MD, Eindhoven, The Netherlands*
[c] *Laboratory of Macromolecular and Organic Chemistry, Department of Chemical Engineering and Chemistry, Eindhoven University of Technology, Post Office Box 513, 5600 MD, Eindhoven, The Netherlands*
[d] *Center for Education and Research on Macromolecules, CESAM Research Unit, University of Liège, Sart-Tilman B6a, B-4000 Liège, Belgium*

Keywords: bio-inspired functional materials, ice recrystallization inhibition, micelles, poly(vinyl alcohol), polyelectrolytes

Abstract

Complex coacervate core micelles (C3Ms) form upon complexation of oppositely charged copolymers. These co-assembled structures are widely investigated as promising building blocks for encapsulation, nanoparticle synthesis, multimodal imaging, and coating technology. Here, the impact on ice growth is investigated of C3Ms containing poly(vinyl alcohol), PVA, which is well known for its high ice recrystallization inhibition (IRI) activity. The PVA-based C3Ms are prepared upon co-assembly of poly(4-vinyl-*N*-methyl-pyridinium iodide) and poly(vinyl alcohol)-*block*-poly(acrylic acid). Their formation conditions, size, and performance as ice recrystallization inhibitors are studied. It is found that the C3Ms exhibit IRI activity at PVA monomer concentrations as low as 1×10^{-3}m. The IRI efficacy of PVA-C3Ms is similar to that of linear PVA and PVA graft polymers, underlining the influence of vinyl alcohol monomer concentration rather than polymer architecture.

Published in: Macromolecular Rapid Communications (2018), vol. 39, n°17, 1700814
DOI: 10.1002/marc.201700814
Status: Postprint (Author's version)

1. Introduction

Complex coacervation is the electrostatically driven, liquid–liquid phase separation that occurs when two aqueous solutions of oppositely charged polyelectrolytes are mixed.[1] Attaching a neutral hydrophilic polymer block to one or both of the polyelectrolytes leads to microphase separation and the formation of micelles, with a complex coacervate core, surrounded by a water-soluble neutral corona.[2] Hence, complex coacervate core micelles (C3Ms) are structures co-assembled in aqueous solutions through electrostatic interactions. This makes them responsive to changes in their environment such as pH, ionic strength, and temperature. These properties render C3Ms applicable for use as multimodal imaging contrast agents,[3] nanogels,[4] nanoreactors,[5] and encapsulation agents.[6]

C3Ms have advantages when used to produce polymer films due to their ease of preparation, fast adsorption, and low desorption.[7] Furthermore, they readily adsorb onto hydrophilic as well as hydrophobic surfaces by exposing their core to the surface while the corona chains extend out into solution.[7a,8] The surface chemistry of C3M-coated substrates can easily be tuned for specific applications, such as antifouling,[7b,9] by changing the corona-forming block. In this work, we use poly(vinyl alcohol), PVA, a well-known ice recrystallization inhibitor,[10] as our corona-forming block. Recently, it was shown that block copolymerization[11] and chain architecture[12] do not affect the ice recrystallization inhibition (IRI) activity of PVA. However, the IRI efficacy of self-assembled structures containing PVA remains a question. To address this challenge we study PVA-based C3Ms formed by poly(4-vinyl-*N*-methylpyridinium iodide), P4VMP, a cationic homopolymer, with poly(vinyl alcohol)-*block*-poly(acrylic acid), PVA-*b*-PAA, a neutral-anionic diblock copolymer, in aqueous solutions. We first determine the critical micelle concentration (CMC) and preferred micelle composition (PMC) at pH 10.5 in 10×10^{-3} m $NaNO_3$ by light scattering. Next, we check whether PVA-based C3Ms inhibit ice recrystallization. A commonly used method to study IRI is the splat assay.[13] Alternatively, to simultaneously view multiple samples, a practical capillary method can be adopted.[14] Here, we determine ice growth rate constants (k_d) over a range of polymer concentrations in the more recently presented sucrose sandwich assay.[15] This method warrants a constant, low ice volume fraction. We find that PVA-based C3Ms effectively inhibit ice recrystallization at vinyl alcohol monomer (VAM) concentrations as low as 1×10^{-3} m. Their activity is comparable to linear chains and PVA bottlebrushes.[12] This indicates that the IRI activity of PVA is dependent on the VAM concentration rather than the polymer architecture. These results unveil that PVA can be formulated into polymeric micelles without loss of IRI activity.

2. Experimental Section

2.1. MATERIALS

Poly(vinyl alcohol)-*b*-poly(acrylic acid), PVA_{273}-*b*-PAA_{353} (M_n = 37 464 g mol^{-1}), was obtained through complete hydrolysis of poly(vinyl acetate)-*b*-poly(acrylonitrile), $PVAc_{273}$-*b*-PAN_{353} (SEC (DMF): M_n = 130 700 g mol^{-1}, Đ = 1.22), which was synthesized by cobalt-mediated radical polymerization as described

Published in: Macromolecular Rapid Communications (2018), vol. 39, n°17, 1700814
DOI: 10.1002/marc.201700814
Status: Postprint (Author's version)

previously.[16] Poly(4-vinyl-*N*-methylpyridinium iodide), $P4VMP_{233}$ (SEC: M_n = 28 000 g mol^{-1}, Đ = 1.2, after quaternization), was purchased from Polymer Source Inc. (Montreal, Canada). The degree of quaternization is >98%.

Sodium nitrate >99% (Agros Organics) was purchased from Fischer Scientific. Sodium hydroxide >98% (Emprove) and hydrogen peroxide (Emprove 35% H_2O_2) were purchased from Merck Millipore Chemicals. Sulfuric acid (Rectapur 95% H_2SO_4) was purchased from VWR. Sucrose ≥99.5% (BioUltra), silanization solution I (≈5% dimethyldichlorosilane in heptane, Selectophore), technical grade acetone and isopropanol, and GE Whatman syringe filters of 0.2 µm pore size with PVDF and PTFE membranes were purchased from Sigma Aldrich. All chemicals were used as received unless indicated otherwise.

2.2. SAMPLE PREPARATION

All stock solutions were prepared in ultrapure water with 10 × 10^{-3} m $NaNO_3$. The pH was adjusted to 10.5 in all solutions using NaOH to ensure full deprotonation of PAA. The polymer stock solutions were prepared at 20 × 10^{-3} m chargeable monomer concentrations, so that after mixing

$$c_{tot} = c_+ + c_- = c_{4VMP} + c_{AA} \quad (1)$$

and dilutions were done with the 10 × 10^{-3} m $NaNO_3$ solution at pH 10.5. The polymer solutions were mixed at the desired mixing ratio which is expressed as the ratio of the molar concentration of positively charged monomers (c_+) to the total concentration of chargeable monomers ($c_+ + c_-$).

$$f_+ = \frac{c_+}{c_+ + c_-} \quad (2)$$

No change in pH was observed after mixing the polymers to produce micellar solutions. All solvents and solutions, except the polymer solutions, were filtered through 0.2 µm syringe filters to remove trace quantities of dust for light scattering experiments. Experiments and sample storage were done at room temperature.

2.3. METHODS

2.3.1. STATIC (SLS) AND DYNAMIC LIGHT SCATTERING (DLS)

Light scattering experiments were performed on an ALV/CGS-3 MD-4 goniometer system, equipped with a 50 mW Nd:YAG laser operating at 532 nm. The temperature was regulated at 20.0 ± 0.2 °C using a Lauda RM6-S refrigerated circulating bath. The light scattering intensity was recorded at various angles between 30° and 150°. Characteristic decay rates (Γ) were obtained from the CONTIN analysis and used to determine the translational diffusion coefficient (D_T) from the slope of Γ versus q^2. We determined the hydrodynamic radius (R_H) of the C3Ms using the Stokes-Einstein relation. The size distribution of the C3Ms was extracted from data measured at 90° using the CONTIN method.

Published in: Macromolecular Rapid Communications (2018), vol. 39, n°17, 1700814
DOI: 10.1002/marc.201700814
Status: Postprint (Author's version)

2.3.2. ICE RECRYSTALLIZATION INHIBITION ASSAY

A 2 µL droplet of sample was sandwiched between two cover slides and placed in a stage attached to a Nikon ECLIPSE Ci-Pol Optical Microscope where the temperature is controlled by a Linkam LTS 420. A thin polycrystalline ice layer was created by rapidly freezing (20 °C min^{-1}) to −40 °C. The temperature was then raised (10 °C min^{-1}) to −7 °C and kept constant for 1 h. Images were taken every 5 min and analyzed using ImageJ and an in-house written Matlab script to obtain the equivalent radius for each ice crystal (details in the Supporting Information). The ice crystal growth rate constants, k_{dc}, were obtained from the temporal increase in the number average radius cubed as described by LSW theory,[15a] according to

$$\langle R_t \rangle^3 = \langle R_0 \rangle^3 + \frac{8\gamma c_\infty v^2 D}{9RT} t = \langle R_0 \rangle^3 + k_d \cdot t \quad (3)$$

Finally, the inhibitory concentration c_i was obtained from $k_d(c)$ as a function of VAM concentration fit to

$$k_{dc} = k_{d0} - \frac{k_{d0}}{1 + \exp\left(\frac{c_i - c}{s}\right)} \quad (4)$$

where k_{d0} is the growth rate constant at zero inhibitor concentration.[15]

2.3.3. ICE NUCLEATION ACTIVITY

We used a homemade setup consisting of a Peltier stage to cool an array of 24 droplets in a controlled environment (Figure S3, Supporting Information). Glass cover slides (32 × 32 mm) were etched with piranha solution (3:1 mixture of sulfuric acid and hydrogen peroxide). The slides were then rinsed with ultrapure water and acetone consecutively, followed by drying with N_2 flow. Then, a hydrophobic surface was obtained by exposing the slides to an ≈5% dimethyldichlorosilane solution for 30 min, which ensures reproducible contact area between the slide and droplets. The slides were rinsed with heptane and dried under nitrogen. Droplets of 1 µL were placed on a slide and cooled at 5 °C min^{-1} until all were frozen, while recording video with a Lumenera Infinity 1. The freezing of individual droplets is signaled by the sudden increase of scattered light by the crystalline phase. Thus, the temperature at which the grayscale intensity suddenly rises is registered as the nucleation temperature (details in the Supporting Information). We performed at least three assays to obtain data for sufficient statistics on the distribution of nucleation temperatures.

3. Results and Discussion

The concentration above which micelles form is known as the critical micelle concentration, CMC. To determine the CMC, we perform SLS experiments at a fixed ionic strength, pH, and mixing ratio while varying c_{tot} from 10×10^{-5} to 20×10^{-3} m. We prepare C3Ms at charge stoichiometry by mixing aqueous solutions of PVA_{273}-*b*-PAA_{353} and $P4VMP_{233}$ at pH 10.5 in 10×10^{-3} m $NaNO_3$ and record the SLS intensity at a fixed scattering angle of 90°. We find a gradual increase in SLS intensity with increasing chargeable

Published in: Macromolecular Rapid Communications (2018), vol. 39, n°17, 1700814
DOI: 10.1002/marc.201700814
Status: Postprint (Author's version)

monomer concentration until it exhibits a sudden jump in between concentrations of 1 and 2 × 10^{-3} m (**Figure** 1A). We attribute this sudden increase in SLS intensity to the transition from small, charged, soluble complexes to C3Ms in solution. Thus, we consider a 1 × 10^{-3} m chargeable monomer concentration as the CMC for this system.

Next, we prepare C3M solutions with c_{tot} = 10 × 10^{-3} m, well above the CMC, at various mixing ratios and a fixed pH = 10.5 and salt concentration of 10 × 10^{-3} m $NaNO_3$. To confirm the presence of micelles and to determine the PMC, we again perform SLS experiments. Upon increasing the fraction of $P4VMP_{233}$ in solution, we observe an increase in SLS intensity which indicates the presence of complexes formed in solution due to electrostatic interactions (Figure 1B). The intensity reaches a maximum around charge stoichiometry where saturation of binding occurs. For this system, we obtain the maximum intensity corresponding to the PMC at f_+ = 0.52. Subsequently, we perform DLS experiments to determine the hydrodynamic radius (R_H) of the C3Ms. We obtain the area normalized size distribution by CONTIN analysis and find a unimodal distribution (Figure 1C). Using the cumulant method we obtain a hydrodynamic radius of R_H = 47.8 ± 1.1 nm. The micelles are furthermore observed to maintain this size for a period of more than ten weeks (Figure S1, Supporting Information).

Figure 1. Light scattering intensity of complexes formed in aqueous solutions (pH = 10.5, 10 × 10^{-3} m $NaNO_3$) by PVA_{273}-*b*-PAA_{353} and $P4VMP_{233}$ as a function of A) chargeable monomer concentration (c_{tot}); arrow indicates the intensity jump attributed to the CMC; B) mixing ratio (f_+); dashed line indicates the PMC (f_+ = 0.52) where saturation of binding occurs; C) area normalized size distribution of C3Ms (○) and C3Ms with 30 wt% sucrose (Δ) at the PMC.

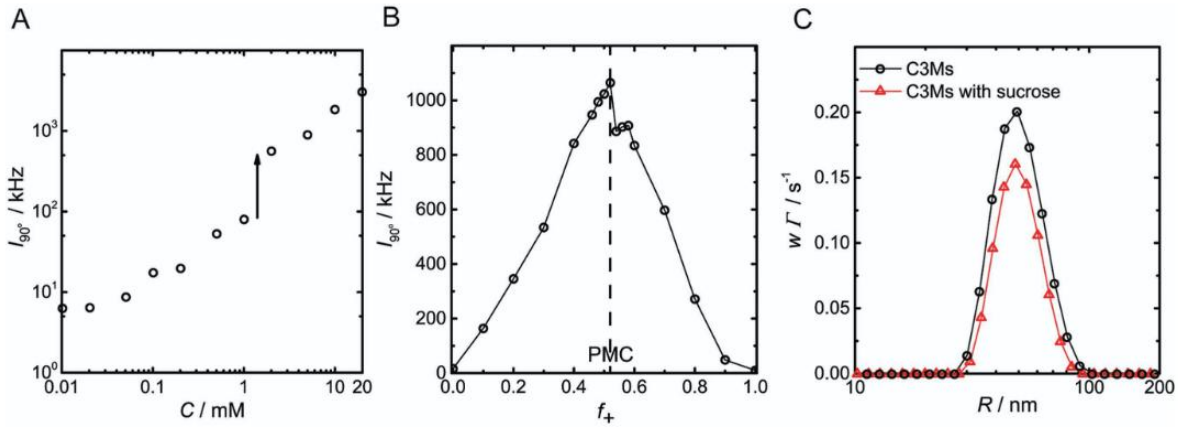

To reliably test whether PVA-containing C3Ms impact ice growth, we measure ice growth rates at low ice volume fractions in 30 wt% sucrose. This high sucrose concentration utilized in a so-called sucrose sandwich assay ensures that individual grains of ice are distinguishable during the entire assay.[15a] Therefore, we first check if sucrose addition influences the size distribution and the hydrodynamic radius of C3Ms by DLS. Figure 1C shows the micellar size distributions determined in both the presence and absence of 30 wt% sucrose at the PMC. We observe no significant changes in the micellar size distributions and the R_H of the C3Ms upon addition of sucrose.

To quantify IRI activity, we perform IRI assays over a range of VAM concentrations from 0.2 to 7.5 × 10^{-3} m. Ice growth rates are drastically decreased when VAM concentrations exceed 0.3 × 10^{-3} m. Full inhibition of ice recrystallization occurs at concentrations above 1 × 10^{-3} m (or 0.044 mg mL^{-1} PVA), which corresponds to c_{tot} = 2.7 × 10^{-3} m chargeable monomer concentration (**Figure** 2A) (see the Supporting Information for representative images). This is in agreement with previously reported results from splat assays on linear PVA of comparable molecular weight: 0.10 mg mL^{-1} for PVA_{246} and

Published in: Macromolecular Rapid Communications (2018), vol. 39, n°17, 1700814
DOI: 10.1002/marc.201700814
Status: Postprint (Author's version)

0.05 mg mL^{-1} for PVA$_{351}$.[17] The IRI efficacy (c_i) is determined from the inflection point of the curve where the ice growth rate is decreased to half of its value at zero inhibitor concentration.[10e,15b] PVA-based C3Ms exhibit c_i = 0.33 × 10^{-3} m, which is similar to linear PVA (c_i = 0.38 × 10^{-3} m) and grafted bottlebrushes (c_i = 0.31 × 10^{-3} m)[12] and is slightly lower than PVA$_{273}$-*b*-PAA$_{353}$ (c_i = 0.47 × 10^{-3} m) (Figure 2B). These results imply that the VAM concentration is the defining factor for IRI activity instead of the architecture of the polymer chain and/or its association state. Note that the block copolymer itself exhibits a somewhat lower IRI activity, which might be due to repulsive interactions between anionic polymer chains.

Figure 2. Normalized ice growth rate constant as a function of VAM concentration of A) C3Ms and B) PVA$_{273}$-*b*-PAA$_{353}$. The IRI efficacy is determined from a fit of Equation 4 to the data, which yields the inhibitory concentration c_i as indicated by the dashed vertical line.

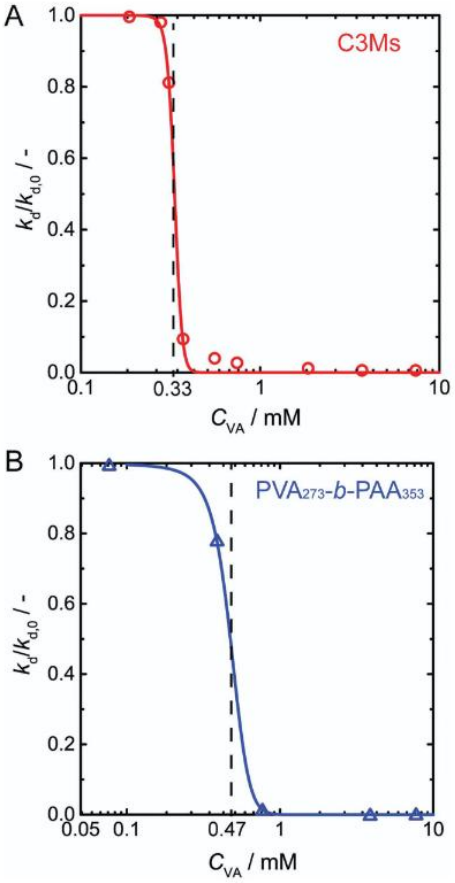

Polymers that inhibit ice growth may also affect ice nucleation. PVA, among other macromolecules, has been reported to promote[10c,f,18] or reduce[19] ice nucleation, depending on the concentration and presence of other compounds like silica nanoparticles. To determine the effect of PVA-based C3Ms on the nucleation of ice crystals, we record the ice nucleation temperatures for aqueous solutions with 7 × 10^{-3} m PVA-C3Ms. For comparison, we also assess 10 × 10^{-3} m PVA$_{273}$-*b*-PAA$_{353}$ and P4VMP$_{233}$ solutions and a reference solution at pH = 10.5 and 10 × 10^{-3} m $NaNO_3$. Using the recorded ice nucleation temperatures, we compute the fraction of frozen droplets as a function of temperature (**Figure** 3A). A comparison of the temperatures at which half of the droplets are frozen ($T_{50\%}$), does not reveal significant differences between the four solutions (Figure 3B). Statistical tests were performed to further quantify this finding (Table S1, Supporting Information). A Shapiro–Wilk test shows that the

Published in: Macromolecular Rapid Communications (2018), vol. 39, n°17, 1700814
DOI: 10.1002/marc.201700814
Status: Postprint (Author's version)

C3M and P4VMP data are not normally distributed, while the two other sets follow a normal distribution. Hence, we adopt a nonparametric test to compare all four distributions (Table S2, Supporting Information). This Mann–Whitney–Wilcoxon test confirms that there is no significant difference between the distributions from the solutions, except for the PVA_{273}-*b*-PAA_{353} and $P4VMP_{233}$ solutions. Nevertheless, we can conclude that neither the block copolymer nor the C3Ms reduce or promote the nucleation of ice crystals in aqueous solutions under the investigated experimental conditions.

Figure 3. A) Frozen fraction as a function of temperature for solutions of C3Ms (7×10^{-3} m), PVA_{273}-*b*-PAA_{353} (10×10^{-3} m), $P4VMP_{233}$ (10×10^{-3} m, negative control), and 10×10^{-3} m $NaNO_3$ as reference. For clarity, 25% of the recorded data points are shown; B) Temperatures at which 50% of droplets are frozen for the four solutions, error bars indicating median absolute deviation.

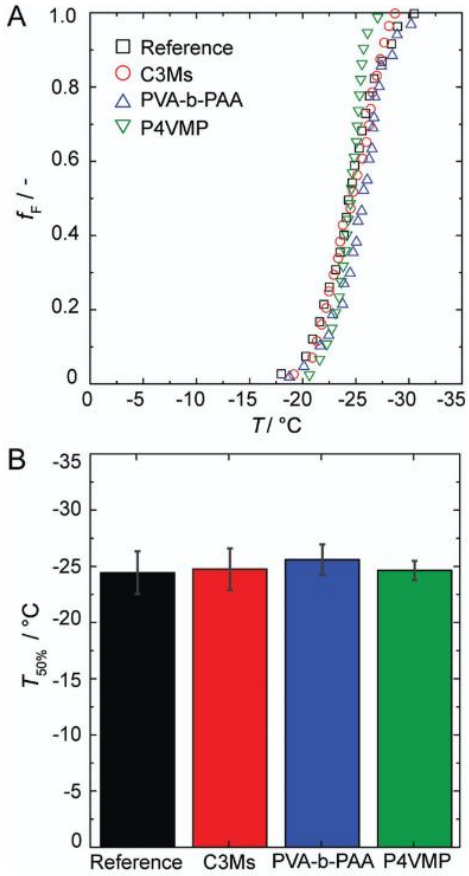

4. Conclusion

Poly(vinyl alcohol)-bearing C3Ms have been prepared upon electrostatically driven co-assembly of PVA_{273}-*b*-PAA_{353} and $P4VMP_{233}$ in aqueous solutions at pH = 10.5 and 10×10^{-3} m $NaNO_3$. C3M characterization by light scattering yields a CMC of c_{tot} ≈1–2 × 10^{-3} m chargeable monomer concentration and a PMC of f_+ = 0.52. A sucrose sandwich assay at f_+ = 0.52 reveals that the PVA-based C3Ms effectively inhibit ice recrystallization even at low VA monomer concentrations of 1×10^{-3} m. We find the inhibitory concentration of the PVA-C3Ms at $c_i = 0.33 \times 10^{-3}$ m, which is comparable to

Published in: Macromolecular Rapid Communications (2018), vol. 39, n°17, 1700814
DOI: 10.1002/marc.201700814
Status: Postprint (Author's version)

the c_i values for linear PVA and PVA bottlebrushes studied previously. This suggests that the VAM concentration is more influential for IRI activity than polymer architecture and association state. Furthermore, we observe that ice nucleation is neither promoted nor reduced by PVA-based C3Ms or by the PVA-*b*-PAA diblock copolymer. These results shed new light on the IRI activity of man-made materials and hold promise for the preparation of C3M-based coatings to control ice adhesion and growth on solid surfaces.

Supporting Information

Supporting Information is available from the Wiley Online Library or from the author.

Acknowledgements

This work was financially supported by the European Union (ERC-2014-StG Contract No. 635928), the Dutch Science Foundation (NWO ECHO Grant No. 712.016.002), and the Dutch Ministry of Education, Culture and Science (Gravity Program 024.001.035). C.D. is research director of F.R.S.-FNRS and thanks FNRS (Belgium) for financial support.

Conflict of Interest

The authors declare no conflict of interest.

References

[1] H. G. Bungenberg de Jong, H. R. Kruyt, Proc. KNAW 1929, 32, 849.

[2] a) A. Harada, K. Kataoka, Macromolecules 1995, 28, 5294; b) A. V. Kabanov, T. K. Bronich, V. A. Kabanov, K. Yu, A. Eisenberg, Macromolecules 1996, 29, 6797; c) M. A. Cohen Stuart, N. A. M. Besseling, R. G. Fokkink, Langmuir 1998, 14, 6846.

[3] D. Vecchione, A. M. Grimaldi, E. Forte, P. Bevilacqua, P. A. Netti, E. Torino, Sci. Rep. 2017, 7, 45121.

[4] M. Takeo, T. Mori, T. Niidome, S. Sawada, K. Akiyoshi, Y. Katayama, J. Colloid Interface Sci. 2013, 390, 78.

[5] a) L. M. Bronstein, S. N. Sidorov, P. M. Valetsky, J. Hartmann, H. Cölfen, M. Antonietti, Langmuir 1999, 15, 6256; b) M. Jaturanpinyo, A. Harada, X. Yuan, K. Kataoka, Bioconjugate Chem. 2004, 15, 344.

[6] a) K. Kataoka, A. Harada, Y. Nagasaki, Adv. Drug Delivery Rev. 2001, 47, 113; b) S. Lindhoud, R. de Vries, R. Schweins, M. A. C. Stuart, W. Norde, Soft Matter 2009, 5, 242.

Published in: Macromolecular Rapid Communications (2018), vol. 39, n°17, 1700814
DOI: 10.1002/marc.201700814
Status: Postprint (Author's version)

[7] a) S. Van Der Burgh, R. Fokkink, A. De Keizer, M. A. C. Stuart, Colloids Surf., A 2004, 242, 167; b) A. M. Brzozowska, Q. Zhang, A. de Keizer, W. Norde, M. A. C. Stuart, Colloids Surf., A. 2010, 368, 96.

[8] I. K. Voets, W. M. De Vos, B. Hofs, A. De Keizer, M. A. C. Stuart, R. Steitz, D. Lott, J. Phys. Chem. B 2008, 112, 6937.

[9] B. Hofs, A. Brzozowska, A. de Keizer, W. Norde, M. A. C. Stuart, J. Colloid Interface Sci. 2008, 325, 309.

[10] a) C. Budke, T. Koop, ChemPhysChem 2006, 7, 2601; b) M. I. Gibson, C. A. Barker, S. G. Spain, L. Albertin, N. R. Cameron, Biomacromolecules 2009, 10, 328; c) H. Y. Wang, T. Inada, K. Funakoshi, S. S. Lu, Cryobiology 2009, 59, 83; d) M. I. Gibson, Polym. Chem. 2010, 1, 1141; e) C. Budke, A. Dreyer, J. Jaeger, K. Gimpel, T. Berkemeier, A. S. Bonin, L. Nagel, C. Plattner, A. L. Devries, N. Sewald, T. Koop, Cryst. Growth Des. 2014, 14, 4285; f) T. Congdon, B. T. Dean, J. Kasperczak-Wright, C. I. Biggs, R. Notman, M. I. Gibson, Biomacromolecules 2015, 16, 2820.

[11] T. R. Congdon, R. Notman, M. I. Gibson, Biomacromolecules 2016, 17, 3033.

[12] L. L. C. Olijve, M. M. R. M. Hendrix, I. K. Voets, Macromol. Chem. Phys. 2016, 217, 951.

[13] C. A. Knight, J. Hallett, A. L. DeVries, Cryobiology 1988, 25, 55.

[14] M. M. Tomczak, C. B. Marshall, J. A. Gilbert, P. L. Davies, Biochem. Biophys. Res. Commun. 2003, 311, 1041.

[15] a) C. Budke, C. Heggemann, M. Koch, N. Sewald, T. Koop, J. Phys. Chem. B 2009, 113, 2865; b) L. L. C. Olijve, A. S. O. Vrielink, I. K. Voets, Cryst. Growth Des. 2016, 16, 4190.

[16] A. Debuigne, J. Warnant, R. Jérôme, I. Voets, A. De Keizer, M. A. C. Stuart, C. Detrembleur, Macromolecules 2008, 41, 2353.

[17] T. Congdon, R. Notman, M. I. Gibson, Biomacromolecules 2013, 14, 1578.

[18] K. Mochizuki, Y. Qiu, V. Molinero, J. Am. Chem. Soc. 2017, 139, 17003.

[19] Z. Zhu, J. Xiang, J. Wang, D. Qiu, Langmuir 2017, 33, 191.